$(N_2)_6Ne_7$: A High Pressure van der Waals Insertion Compound

Thomas Plisson,* Gunnar Weck, and Paul Loubeyre
CEA, DAM, DIF, F-91297 Arpajon, France
(Received 12 April 2014; published 11 July 2014)

The binary phase diagram of N_2-Ne mixtures has been measured at 296 K by visual observation and Raman spectroscopy. The topology of the phase diagram points to the existence of the stoichiometric compound $(N_2)_6Ne_7$. Its structure has been solved by single-crystal synchrotron x-ray diffraction. The N_2 molecules form a guest lattice that hosts the Ne atoms. This insertion compound can be viewed as a clathrate with the centers of the N_2 molecules forming distorted dodecahedron cages, each enclosing 14 Ne atoms. Remarkably, the $(N_2)_6Ne_7$ compound is somehow the first clathrate organized by the quadrupolar interaction.

DOI: 10.1103/PhysRevLett.113.025702 PACS numbers: 64.70.kt, 07.35.+k, 61.50.Ks, 62.50.-p

High pressure modifies substantially the microscopic interactions in the condensed phase and it is inimical to the covalent bonds [1]. This is at the origin of the recently discovered high pressure solid-state chemistry of light element gas molecules. For example, solid molecular nitrogen has been transformed into a single bonded polymeric form of nitrogen [2], solid oxygen into an extended molecular metal [3], and O_2-N_2 mixtures into a $NO^+NO_3^-$ ionic solid [4]. A second remarkable observation is that simple molecules interacting via van der Waals interactions can auto-organize under pressure into stoichiometric solids, called van der Waals compounds. The possibility to couple these two high pressure phenomena in order to tune the microscopic arrangement, the stoichiometry, and the formation of new bonds in simple molecular mixtures opens a promising path to developing novel materials potentially recoverable at ambient conditions [5].

The ubiquity of van der Waals compounds under pressure contrasts with their absence in cryocrystals, making pressure a powerful driving force for self-assembly of molecular compounds. Most of the van der Waals compounds discovered so far are in the form of Laves phases such as $NeHe_2$ [6], $Ar(H_2)_2$ [7], $CH_4(H_2)_2$ [8], or $Xe(O_2)_2$ [9]. Their stability is explained by analogy with intermetallic compounds [10] and colloidal systems [11] in terms of binary crystals of hard spherelike particles. The efficient packing and configurational entropy contributions have to be taken into account to quantify such a stability. Pressure enables to maximize both terms, whereas the term of entropy is negligible in the low temperature compaction. Other classes of van der Waals compounds have been discovered. In $(N_2)_{11}He$ [12], the structure is explained by the substitution of two N_2 molecules by He atoms on sites 6 b of the ϵ-N_2 structure [13]. In a few cases, though, unexpected stoichiometries have been observed, such as $(O_2)_3(H_2)_4$ [14] or $Xe(H_2)_7$ [15], but their structures and the reason for their stability are still unclear. As a matter of fact, the interplay between packing and the anisotropic components of the van der Waals interactions, such as the quadrupole-quadrupole interaction, to stabilize new kinds of van der Waals compounds, has been hardly investigated. The quadrupole-quadrupole interaction, proportional to $1/r^5$ (r being the nearest-neighbor intermolecular distance), which therefore increases under pressure, is responsible for the rich polymorphism of pure solid N_2 under pressure [16].

In this Letter, we demonstrate the existence of a new type of high pressure van der Waals compound discovered in N_2-Ne mixtures. We present the determination of the N_2-Ne binary phase diagram which led to the identification of the $(N_2)_6Ne_7$ compound. We describe the characterization of its structure by single crystal x-ray diffraction. This compound has a remarkably complex guest-host structure in which N_2 molecules form large dodecahedron cages enclosing the Ne atoms. This structure is the first van der Waals clathrate ever observed and opens a route for the development of a new family of host-guest systems in high pressure molecular mixtures. This result may also be relevant for colloid mixtures in which the space filling of hard spheres explains their Laves phases [17] and the existence of quadrupolar interaction produces complex structures such as the house-of-cards structure in clay [18]. Finally, the $(N_2)_6Ne_7$ compound offers a pathway to observing other extended nitrogen allotropic structures [19] at very high pressure, among which is an intriguing diamondoid structure formed by N_{10} cage units [20].

The binary phase diagram of N_2-Ne mixtures is up to now unknown. It has not been studied at ambient pressure by varying temperature [21] and it has been only sketched at 296 K by studying three concentrations in a diamond anvil cell [22]. Interestingly, though, this first high pressure Raman spectroscopy study has suggested the possible formation of compounds in solid N_2-Ne mixtures. We have performed a detailed measurement of the N_2-Ne binary

diagram at 296 K by studying 16 different concentrations. The experimental procedure is similar to the one used in our previous measurements on mixtures [6,9]. The membrane diamond anvil cell equipped with 300 μm flat anvil culets and an inox-301 gasket was loaded at room temperature in a high pressure vessel, typically under a pressure of 20 MPa and after sufficient homogenization time (~12 h). The initial concentration of the mixture was estimated from the partial pressures of the gases, corrected with the virial coefficients. The pressure was measured with the ruby luminescence gauge. The uncertainties in pressure and in concentration are ± 0.05 GPa and ± 1 mol %, respectively. The N_2-Ne binary phase diagram presented in Fig. 1(a) has been determined mainly by visual observation through a microscope visualization associated with the pressure measurement. Solid-fluid equilibrium could easily be observed. At a given concentration, the liquidus transition point was measured by pinpointing the pressure of disappearance of a single crystal in equilibrium with the fluid upon decreasing pressure.

As shown in Fig. 1(a), the N_2-Ne binary diagram is of the eutectic type with a total miscibility of N_2 and Ne in the fluid phase. Interestingly, the liquidus line in between the two eutectic points, at 42 and 59 mol % Ne, is of a convex shape with a minimum at 54 mol % Ne. This topology of the liquidus line points to the existence of a stoichiometric compound at this concentration. The fact that congruent melting is observed at 54 mol % Ne, whereas an increasingly contrasted solid-solid phase separation is observed upon departing from this concentration confirms this hypothesis. Therefore, the stoichiometric compound corresponds to the formula $(N_2)_6Ne_7$. Raman spectroscopy of the vibron modes of N_2 has been performed to obtain the spectroscopic signature of $(N_2)_6Ne_7$. The laser used in our setup has a wavelength of 491.5 nm and the spectral resolution is 3 cm^{-1}. As shown in Fig. 1(b), $(N_2)_6Ne_7$ exhibits two Raman vibron modes with frequencies in between and significantly different from the ones of the two vibron modes measured at the same pressure in pure solid N_2. Below 11 GPa, the vibrons are close in frequency and not resolved in our setup. Raw Raman spectra are presented in the online Supplemental Material [24]. Raman spectroscopy has also been useful to complement visual observation and show that the solubilities of N_2 in solid Ne and Ne in solid N_2 are less than 2 mol %, this being the smaller concentration for which we were able to observe phase separation.

It should be mentioned that large metastability is observed in the formation of the compound. Between the two eutectic points, the fluid can be overpressured. Solid-solid phase separation between pure neon and pure nitrogen has sometimes been observed as if the compound did not exist, before the compound eventually appears. It will be shown below that the structure of the $(N_2)_6Ne_7$

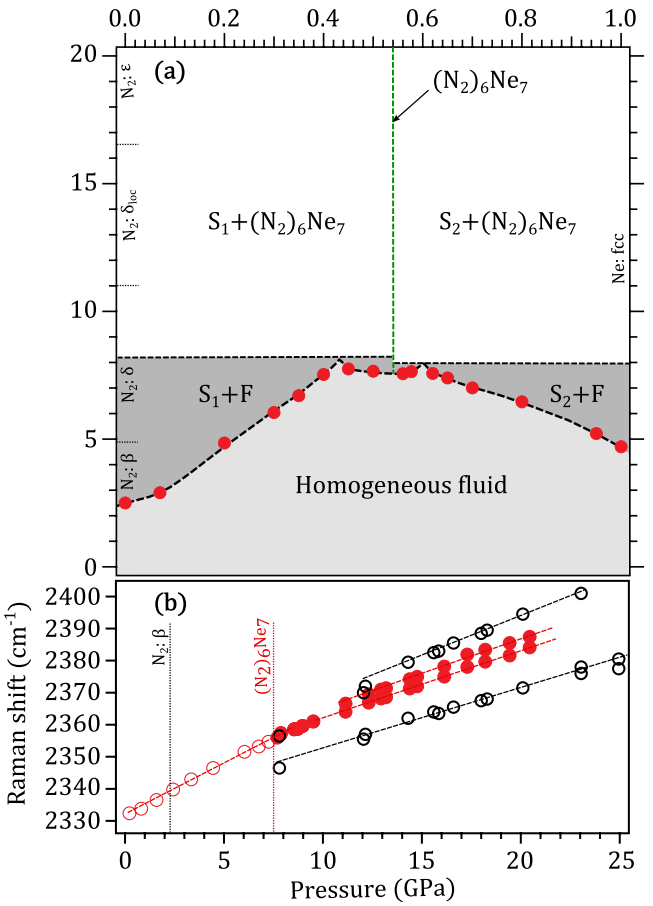

FIG. 1 (color online). (a) Binary phase diagram of the N_2-Ne mixture at 296 K plotted as pressure vs Ne concentration. The solid S_1 stands for the rich N_2 solid phase, S_2 for the rich Ne solid phase, and F for the fluid phase. On the vertical axis, we indicate the domains of existence for the pure constituents. The mutual solubilities of N_2 and Ne in the solid phase are less than 2%. The red dots form the measured liquidus. The van der Waals compound is found at $x_{Ne} = 0.54$. (b) Evolution with pressure of the Raman frequency of the N_2 vibrons in a N_2-Ne mixture at $x_{Ne} = 0.54$. The red circles are obtained in $(N_2)_6Ne_7$. The empty red circles are obtained in the fluid. Below 11 GPa in the solid phase, the two vibrons are not resolved by our Raman setup. The error bars are smaller than the size of the circles. Empty black circles are the data for pure N_2 from Schneider *et al.* [23]. The vertical dashed lines indicate the melting pressures for pure N_2 and $(N_2)_6Ne_7$.

van der Waals compound is complex and its probability to nucleate in the fluid is likely to be quite low. The compound is obtained by compressing the sample above 9.6 GPa, pressure at which it is in equilibrium in the solid phase with solid Ne and/or solid N_2. Then by decreasing the pressure below the two eutectic points, the end component solids are melting and a pure compound can be stabilized. From a small grain of $(N_2)_6Ne_7$ at its melting point, a single crystal can be grown. A typical single crystal, grown from a 45 mol % mixture, is shown in Fig. 2(b). The synthesis of a

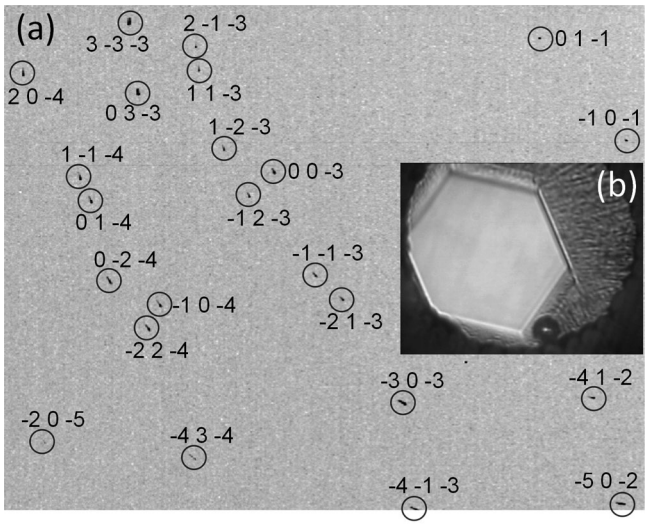

FIG. 2. (a) Composite image, obtained by adding 120 image plates, showing the indexed Bragg peaks of the single crystal of $(N_2)_6Ne_7$ at 8 GPa. For clarity, only a part of the full image is presented, and the observed peaks are circled. (b) Photograph of a single crystal of $(N_2)_6Ne_7$ surrounded by the solid-solid phase separation between pure solid N_2 and $(N_2)_6Ne_7$, grown from the N_2-Ne mixture with initial concentration $x_{Ne} = 0.45$. The hexagonal faceting of the macroscopic crystal reveals the underlying hexagonal structure of the $(N_2)_6Ne_7$ compound.

high quality single crystal has been essential to determining the structure of $(N_2)_6Ne_7$.

We have performed single-crystal angular dispersive x-ray diffraction measurements at the ID09 beam line of the European Synchrotron Radiation Facility (ESRF), using a monochromatic beam with a wavelength of 0.414 036 Å. Data were collected on a single crystal at 8.0 GPa grown from a 54 mol % Ne mixture, thus filling the whole sample chamber. A total of 225 reflections have been measured. Figure 2(a) illustrates the quality of the collected diffraction signal. Indexing of the observed reflections with the CrysAlisPro software (Oxford Diffraction) gives a hexagonal unit cell with lattice parameters: $a = 14.3996(8)$ Å and $c = 8.0940(3)$ Å at 8.0 GPa. Using the structure solution software SIR2011 [25] and final refinement using SHELXL2013 [26], the solved structure is found to belong to the $R\bar{3}m$ space group, with seven nonequivalent atoms: four neon and three nitrogen atoms. The refined coordinates are reported in Table I along with the final R-factor. In the refinement, the N atoms of the N_2 molecules were considered independent. It was shown that for the N_2 molecules, the presence of tightly bonded core electrons overshadow the changes in scattering due to the covalent bond affecting the valence electrons [27]. In the situation of spherical disorder for the N_2 molecule, a specific scattering form factor was used [16,28]. In our study, treating the molecule as isolated atoms was satisfactory, resulting in small residual electron density between $-0.26\ e/Å^3$ and $+0.22\ e/Å^3$. The intramolecular N-N distances are,

TABLE I. Refined atomic positions of the $(N_2)_6Ne_7$ structure with $R\bar{3}m$ symmetry, at 8.0 GPa and 296 K. The cell parameters are $a = 14.3996(8)$ Å and $c = 8.0940(3)$ Å. We give the figures of merit of the refinement, defined by $R = \sum ||F_c| - |F_o|| / \sum |F_o|$ and $R_{int} = \sum ||F_c|^2 - |F_o|^2| / \sum |F_o|^2$, where $|F_c|$ and $|F_o|$ are, respectively, the calculated and observed amplitude of the structure factors of the reflections. Among the 225 reflections collected, 184 reflections have $|F_o| > 4\sigma$ where σ is the error on $|F_o|$. We obtain $R(|F_o| > 4\sigma) = 0.0491$, $R(\text{all}) = 0.0587$, and $R_{int} = 0.1499$.

	x	y	z	Occupation	U_{iso}(Å^2)
Ne_1	0.211 53	0.605 76	0.423 79	1/2	0.0502
Ne_2	0.333 33	0.666 67	−0.33333	1/12	0.0444
Ne_3	−0.134 00	0.433 00	0.275 45	1/2	0.0519
Ne_4	0.333 33	0.666 67	0.166 67	1/12	0.0478
N_1	0.112 91	0.556 46	0.075 05	1/2	0.0696
N_2	−0.074 05	0.293 58	0.140 00	1	0.0676
N_3	0.068 55	0.534 27	0.168 70	1/2	0.0762

respectively, 0.938 Å and 0.958 Å for the N_1-N_3 and N_2-N_2 molecules. These distances are calculated by taking the average position of each atom separately, and differ from the molecular distance because of thermal motion [29]. If we correct these distances by assuming a rigid libration of the molecules, the distances change to 1.093 and 1.099 Å, respectively. These distances are in good agreement with previously measured values: 1.098 Å in the gas phase [30], 1.0 to 1.06 Å in the δ-N_2 phase [16], and 1.097 Å in the $(N_2)_{11}He$ compound [13].

The structure of the $(N_2)_6Ne_7$ compound, presented in Fig. 3, offers a complex arrangement of N_2 molecules and Ne atoms. The view along the [001] direction [Fig. 3(a)] reveals the presence of columns of Ne atoms surrounded by a structure of nitrogen molecules. The structure of a Ne column is represented in Fig. 3(b). One can distinguish [Fig. 3(b), [b1]] two motifs alternating in the [001] direction: (a) one Ne atom, labeled Ne_4 in Table I, surrounded by six N_2 molecules in a benzenelike structure and (b) thirteen Ne atoms surrounded by twelve N_2 molecules. Interestingly, the N_2 molecules were found to be oriented at 8.0 GPa and 296 K, unlike in pure δ-nitrogen in which N_2 molecules present spherelike or disklike disorder [16].

Furthermore, the nitrogen structure surrounding the Ne atoms can be seen as an open cagelike structure. In Fig. 3(b), [b2] and Fig. 3(b), [b3] are drawn the nearest-neighbor distances between the centers of the N_2 molecules, for distances ranging from 3.06 to 3.68 Å at 8.0 GPa. The surfaces supported by the molecules are colored in red, to emphasize the presence of distorted pentagons, forming a cage. However, this nitrogen structure is not fully closed, which is mainly due to the presence of the two isolated Ne atoms at the top and bottom of the cage [see Fig. 3(b), [b2]

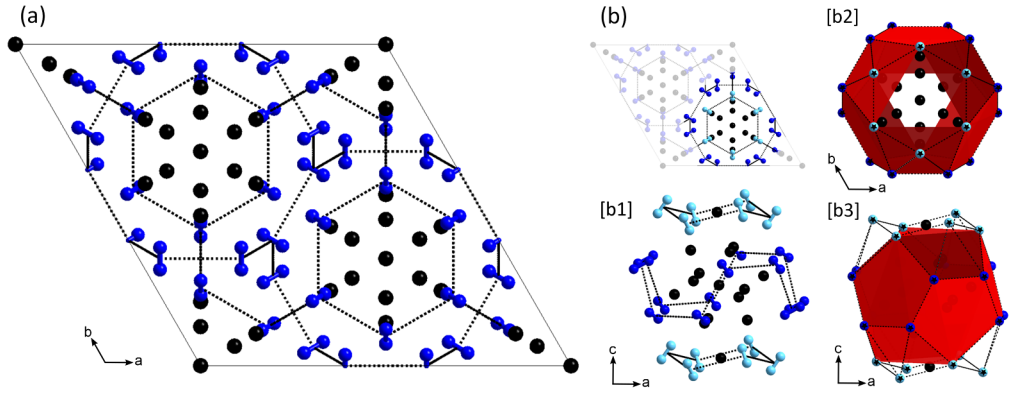

FIG. 3 (color online). Crystal structure of the $(N_2)_6Ne_7$ compound. Neon and nitrogen are represented by black and blue spheres, respectively. The black dashed lines join the centers of adjacent N_2 molecules. (a) Unit cell represented along the c axis ([001] direction). (b) Details of the Ne structure and of their nitrogen surroundings. In [b1], only N_2-N_2 distances ranging from 3.05 to 3.16 Å at 8.0 GPa are shown. The view is slightly rotated from a pure b-axis view to show the 3D perspective. In [b2] and [b3], N_2-N_2 distances ranging from 3.05 to 3.68 Å at 8.0 GPa are shown. The red planes show the surfaces supported by the centers of the N_2 molecules. They form a cagelike structure that can be seen as a distortion from a dodecahedron, due to the presence of the top and bottom Ne atoms which open the cage. For clarity, only the centers of the molecules are represented (blue spheres marked with a black star). The view in [b2] is along the c axis, whereas [b3] is slightly rotated from a pure b-axis view.

and Fig. 3(b), [b3]]. It results, in our structure, in the top and bottom vertices of the polyhedron being split apart and in the opening of the structure. In Fig. 3(b), [b2], we can see, at the top (or bottom) of the polyhedron, that a unique missing N_2 molecule could complete the three incomplete pentagons, while three N_2 molecules are out of the polyhedron faces. It shall be noted that the full pentagons are not regular in edge length.

This cage structure of nitrogen filled with Ne atoms shares the characteristics of a clathrate. In clathrate hydrates the hydrogen bonded water framework forms cages that can trap the guest molecules [31]. In group IV clathrates, the host lattice contains hexagonal and pentagonal rings fused together by sp^3 bonding to form large cages; and a carbon clathrate with dodecahedron C_{20} has been synthesized [32]. In the present clathrate structure, though, the nitrogen cages are shaped by the quadrupole-quadrupole interaction and they enclose a large amount of guest atoms. The fact that van der Waals interactions could be the driving force for the self-organization of the N_2-Ne mixture into such an open compound at high pressure was highly unexpected. The prediction of this structure from calculations, either with *ab initio* simulations or by assuming intermolecular interactions, could be a challenging test for calculation-based engineering of new materials at high pressure.

In summary, by precisely exploring the N_2-Ne binary phase diagram under pressure, we have identified a van der Waals compound of a new kind, with stoichiometry $(N_2)_6Ne_7$. The structure was determined by single crystal x-ray diffraction and turns out to be a cagelike arrangement of N_2 molecules stabilized by quadrupolar interactions. The compression of this compound in the megabar range will now be extremely interesting. This system is ideally suited to provide new insights into the synthesis mechanisms of polymeric nitrogen.

We acknowledge the ESRF for provision of beam time under proposals HC1077 on the ID09 beam line. We wish to thank M. Hanfland, L. Bezacier, and C. Pépin for their help with x-ray-diffraction experiments and F. Datchi for helpful discussions.

*thomas.plisson@cea.fr

[1] W. Grochala, R. Hoffmann, J. Feng, and N. Ashcroft, Angew. Chem., Int. Ed. **46**, 3620 (2007).
[2] M. I. Eremets, A. G. Gavriliuk, I. A. Trojan, D. A. Dzivenko, and R. Boehler, Nat. Mater. **3**, 558 (2004).
[3] G. Weck, S. Desgreniers, P. Loubeyre, and M. Mezouar, Phys. Rev. Lett. **102**, 255503 (2009).
[4] D. Sihachakr and P. Loubeyre, Phys. Rev. B **74**, 064113 (2006).
[5] P. F. McMillan, Nat. Mater. **1**, 19 (2002).
[6] P. Loubeyre, M. Jean-Louis, R. LeToullec, and L. Charon-Gérard, Phys. Rev. Lett. **70**, 178 (1993).
[7] P. Loubeyre, R. Letoullec, and J.-P. Pinceaux, Phys. Rev. Lett. **72**, 1360 (1994).
[8] M. S. Somayazulu, L. W. Finger, R. J. Hemley, and H. K. Mao, Science **271**, 1400 (1996).
[9] G. Weck, A. Dewaele, and P. Loubeyre, Phys. Rev. B **82**, 014112 (2010).
[10] W. Hume-Rothery, R. E. Smallman, and C. W. Haworth, *The Structure of Metals and Alloys* (The Institute of Metals, London, 1969).
[11] A.-P. Hynninen, L. Filion, and M. Dijkstra, J. Chem. Phys. **131**, 064902 (2009).
[12] W. L. Vos, L. W. Finger, R. J. Hemley, J. Z. Hu, H. K. Mao, and J. A. Schouten, Nature (London) **358**, 46 (1992).

[13] S. Ninet, G. Weck, P. Loubeyre, and F. Datchi, Phys. Rev. B **83**, 134107 (2011).
[14] P. Loubeyre and R. LeToullec, Nature (London) **378**, 44 (1995).
[15] M. Somayazulu, P. Dera, A. F. Goncharov, S. A. Gramsch, P. Liermann, W. Yang, Z. Liu, H.-K. Mao, and R. J. Hemley, Nat. Chem. **2**, 50 (2010).
[16] G. W. Stinton, I. Loa, L. F. Lundegaard, and M. I. McMahon, J. Chem. Phys. **131**, 104511 (2009).
[17] M. D. Eldridge, P. A. Madden, and D. Frenkel, Nature (London) **365**, 35 (1993).
[18] M. Dijkstra, J. P. Hansen, and P. A. Madden, Phys. Rev. Lett. **75**, 2236 (1995).
[19] F. Zahariev, S. V. Dudiy, J. Hooper, F. Zhang, and T. K. Woo, Phys. Rev. Lett. **97**, 155503 (2006).
[20] X. Wang, Y. Wang, M. Miao, X. Zhong, J. Lv, T. Cui, J. Li, L. Chen, C. J. Pickard, and Y. Ma, Phys. Rev. Lett. **109**, 175502 (2012).
[21] V. G. Manzheli, A. I. Prokhvatilov, I. Y. Minchina, and L. D. Yantsevich, *Handbook of Binary Solutions of Cryocrystals* (Begell House, New York, 1996).
[22] M. E. Kooi and J. A. Schouten, Phys. Rev. B **60**, 12635 (1999).
[23] H. Schneider, W. Hafner, A. Wokaun, and H. Olijnyk, J. Chem. Phys. **96**, 8046 (1992).
[24] See Supplemental Material at http://link.aps.org/supplemental/10.1103/PhysRevLett.113.025702 for a presentation of the corresponding raw Raman spectra.
[25] M. C. Burla, R. Caliandro, M. Camalli, B. Carrozzini, G. L. Cascarano, C. Giacovazzo, M. Mallamo, A. Mazzone, G. Polidori, and R. Spagna, J. Appl. Crystallogr. **45**, 357 (2012).
[26] G. M. Sheldrick, Acta Crystallogr. Sect. A **64**, 112 (2008).
[27] P. F. Morrisson and C. J. Pings, J. Chem. Phys. **56**, 280 (1972).
[28] D. T. Cromer, R. L. Mills, D. Schiferi, and L. A. Schwalbe, Acta Crystallogr. Sect. B **37**, 8 (1981).
[29] W. R. Busing and H. A. Levy, Acta Crystallogr. **17**, 142 (1964).
[30] R. LeSar, S. Ekberg, L. Jones, R. Mills, L. Schwalbe, and D. Schiferl, Solid State Commun. **32**, 131 (1979).
[31] W. L. Mao, C. A. Koh, and E. D. Sloan, Phys. Today **60**, No. 10, 42 (2007).
[32] Z. Iqbal, Y. Zhang, H. Grebel, S. Vijayalakshmi, A. Lahamer, G. Benedek, M. Bernasconi, J. Cariboni, I. Spagnolatti, R. Sharma, F. Owens, M. Kozlov, K. Rao, and M. Muhammed, Eur. Phys. J. B **31**, 509 (2003).